Atherosclerosis 286 (2019) 88–96

Contents lists available at ScienceDirect

Atherosclerosis

journal homepage: www.elsevier.com/locate/atherosclerosis

Identification of circular RNA *Hsa_circ_0001879* and *Hsa_circ_0004104* as novel biomarkers for coronary artery disease

Laiyuan Wang[a,*,1], Chong Shen[b,1], Yanyu Wang[a], Tianyu Zou[a], Huijuan Zhu[a], Xiaomei Lu[a], Lin Li[a], Bin Yang[a], Jichun Chen[a], Shufeng Chen[a], Xiangfeng Lu[a], Dongfeng Gu[a]

[a] Key Laboratory of Cardiovascular Epidemiology & Department of Epidemiology, State Key Laboratory of Cardiovascular Disease, Fuwai Hospital, National Center for Cardiovascular Diseases, Chinese Academy of Medical Sciences and Peking Union Medical College, Beijing, 100037, China
[b] Department of Epidemiology, School of Public Health, Nanjing Medical University, 101 Longmian Avenue, Jiangning, Nanjing, 211166, China

HIGHLIGHTS

- We offered a transcriptome-wide overview of aberrantly expressed circRNAs in CAD patients.
- hsa_circ_0001879 and hsa_circ_0004104 were identified as novel circRNA biomarkers for diagnosing CAD.
- Hsa_circ_0004104 might contribute to the pathogenesis of atherosclerosis and CAD by regulating atherosclerosis related genes expression.

ARTICLE INFO

Keywords:
Coronary artery disease
Circular RNA
Hsa_circ_0001879
Hsa_circ_0004104
Biomarker

ABSTRACT

Background and aims: The role of circular RNAs (circRNAs) in coronary artery disease (CAD) remains elusive. The aim of the present study was to profile circRNAs expression in CAD patients and assess diagnostics biomarkers for CAD.

Methods: The circRNA profiles of 24 CAD patients and 7 controls were assessed by microarray. The expression levels of candidate circRNAs were further verified by qRT-PCR in large cohorts. Logistic regression analysis and receiver operating characteristic were conducted to assess the diagnostic value. Gain-of-function approach was used to determine the functional significance of validated circRNA in THP-1-derived macrophages.

Results: A total of 624 circRNAs and 171 circRNAs were significantly upregulated and downregulated, respectively, in CAD patients relative to controls. Hsa_circ_0001879 and hsa_circ_0004104 were validated to be significantly upregulated in large cohorts. The receiver operating characteristics analysis of hsa_circ_0001879 and hsa_circ_0004104 in CAD patients and controls showed that the area under curve was 0.703 (95% confidence interval: 0.656–0.750; $p < 0.001$) and 0.700 (95% confidence interval: 0.646–0.755; $p < 0.001$), respectively. The combination of hsa_circ_0001879 and hsa_circ_0004104, together with CAD risk factors, had the better performance to discriminate CAD patients from healthy controls. Overexpression of hsa_circ_0004104 resulted in dysregulation of atherosclerosis-related genes in THP-1-derived macrophages.

Conclusions: We offered a transcriptome-wide overview of aberrantly expressed circRNAs in CAD patients and identified two novel circRNA biomarkers to diagnose CAD. Upregulation of hsa_circ_0004104 might contribute to the pathogenesis of CAD.

1. Introduction

Coronary artery disease (CAD) is one of the most common forms of cardiovascular diseases and becomes a severe threat to public health [1]. Although current diagnosis and treatment strategies of CAD, including medications and surgery methods, have been developing,

Abbreviations: ApoA I, apolipoprotein AI; AUC, area under receiver–operator characteristic curve; CAD, coronary artery disease; circRNAs, circular RNAs; eRNA, extracellular RNA; FC, fold changes; GAPDH, glyceraldehyde 3-phosphate dehydrogenase; IDO1, indoleamine 2,3-dioxygenase 1; PBMCs, peripheral blood mononuclear cells; ROC, receiver–operator characteristic

* Corresponding author. Department of Epidemiology, State Key Laboratory of Cardiovascular Disease, Fuwai Hospital, National Center for Cardiovascular Diseases, Chinese Academy of Medical Sciences and Peking Union Medical College, 167 Beilishi Road, Beijing, 100037, China.
E-mail address: wanglaiyuandw@163.com (L. Wang).
[1] These authors contributed equally to this work as first authors.

https://doi.org/10.1016/j.atherosclerosis.2019.05.006
Received 28 October 2018; Received in revised form 4 March 2019; Accepted 8 May 2019
Available online 09 May 2019
0021-9150/

mortality has remained dismal and prognosis ineligible [2]. The main reason accounting for this discrepancy is lack of a highly efficient and convenient diagnosis of CAD. Therefore, it is urgent to search for sensitive and specific biomarkers for early diagnosis of CAD.

Circular RNAs (circRNAs) are a class of endogenous RNA composed of transcripts from exons, introns, or both to form a closed continuous loop [3]. Because circRNAs do not have 5′ or 3′ ends, they are free of exonuclease-mediated degradation and more stable than most linear RNAs [4]. CircRNAs regulate gene expression through multiple mechanisms [5]. They may act as “miRNA sponges”, which can competitively bind to microRNAs (miRNAs), thus suppressing miRNA activity and participating in post-transcriptional regulation of miRNA target genes [6].

Recently, studies have shown that circRNAs are implicated in a variety of pathological conditions, including myocardial infarction [7], heart failure [8], colorectal cancer [9]. Due to their stability and sequence conservation characteristics, circRNAs have been reported to become a novel class of biomarkers for human diseases [10–13]. However, expression profiles and the biological functions of circRNAs in CAD remain elusive.

In this study, we profiled transcriptome-wide circRNAs expression in peripheral blood mononuclear cells (PBMCs) of CAD patients and controls, validated two circRNAs of a four-circRNA signature in a large cohort, and found that hsa_circ_0001879 and hsa_circ0004104 could be diagnostic biomarkers for CAD. Gain-of-function approach was used to explore the functional significance of hsa_circ0004104 in human monocytic cell line (THP-1)-derived macrophages.

2. Materials and methods

2.1. Study population

From January 2011 to January 2014, a total of 436 CAD male patients were recruited from Fuwai Hospital in Beijing. According to the ACC/AHA classification, diagnosis of CAD was based on the final diagnosis at discharge, including acute myocardial infarction, unstable angina and stable angina with > 50% stenosis of the left main coronary trunk or > 75% stenosis in a major epicardial artery by coronary angiography. A total of 297 age-matched male controls free from CAD or stroke were recruited from Shijingshan community and Henan province from September 2013 to June 2014. CAD cases and controls with congenital heart disease, rheumatic valvular disease, cardiomyopathy, stroke, diabetes mellitus, malignant tumors, acute or chronic infected diseases, and severe liver or kidney dysfunction were excluded from the study. Twenty-four CAD patients and 7 healthy controls were selected from 436 CAD patients and 297 healthy controls for circRNA microarray assay, and 412 CAD patients and 290 healthy controls were used as replication population for the validation of differentially expressed circRNAs.

The protocol of this study was approved by the Ethics Committee of Fuwai Hospital in Beijing, China. Written informed consent was obtained from all patients or their families under the Declaration of Helsinki.

2.2. PBMCs isolation

Overnight fasting blood samples were drawn from all participants by venipuncture. PBMCs were isolated from the middle white monolayer by density gradient centrifugation using Lymphocyte Separation Medium (TBD, Tianjin, China), then preserved in TRIzol reagent (Invitrogen, Carlsbad, CA, USA) at −80 °C.

2.3. RNA isolation and qRT-PCR assay

Total RNA from PBMCs or THP-1-derived macrophages was extracted using TRIzol reagent and purified with TURBO DNA-free (Ambion, Austin, USA) according to the manufacturer's protocol. RNA quantity was assessed using NanoDrop 2000 (NanoDrop Products, Wilmington, DE). cDNA was synthesized using Transcriptor First Strand cDNA Synthesis Kit (Roche, Basel, Switzerland), and realtime quantitative reverse transcription polymerase chain reaction (qRT-PCR) was performed using ABI SYBR master mix with ABI Prism 7900 HT Fast Real-Time PCR System (Applied Biosystems, Foster City, USA). qRT-PCR was also used to validate differentially expressed mRNAs selected from the profiling data of THP-1-derived macrophages infected with AAV-DJ-hsa_circ_0004104. Glyceraldehyde 3-phosphate dehydrogenase (GAPDH) was used for internal normalization. Primer sequences are listed in Supplementary Table 1. The relative fold-change was calculated using the $2^{-\Delta\Delta Ct}$ method normalized to *GAPDH*. All experiments were performed in triplicate.

2.4. CircRNA microarray analysis

CircRNA microarray assay was performed by Shanghai Biotechnology Corporation (Shanghai, P.R. China) with SBC human circRNA array V1.0 (4 × 180 K) according to the manufacturer's procedures. Briefly, each RNA sample was purified with RNeasy Mini Kit (Qiagen, GmBH, Germany), and quantified by NanoDrop ND-2000 (Thermo Scientific). RNA integrity was assessed using Agilent Bioanalyzer 2100 (Agilent Technologies). Then, RNA samples of each group were used to generate fluorescence labeled cRNA targets for circRNA array. The labeled cRNA targets were then hybridized with the slides. After hybridization, slides were scanned on the Agilent Microarray Scanner (Agilent technologies, Santa Clara, CA, US). Data were extracted with Feature Extraction software 10.7 (Agilent technologies, Santa Clara, CA, US). Raw data were normalized with the Quantile algorithm of limma package in the R program. Fold-change ≥1.5 and a p-value < 0.05 were considered as criteria for selecting differentially expressed genes. The microarray data analyzed in this study have been deposited in the NCBI GEO database under accession number GSE115733 (https://www.ncbi.nlm.nih.gov/geo/query/acc.cgi?acc=GSE115733).

2.5. Macrophage differentiation, AAV infection and mRNA expression profiling

Human monocytic THP-1 cells were obtained from ATCC (Manassas, VA) and maintained in RPMI 1640 medium (R8758, Sigma-Aldrich, St. Louis, MO, USA) supplemented with 10% fetal bovine serum (FBS, Gibco, Carlsbad, CA), 1% penicillin/streptomycin solution (Gibco, Carlsbad, CA) for all experiments. THP-1 monocytes were maintained at 37 °C in a humidified chamber containing 5% CO_2, seeded into 12 wells culture plates and incubated with 100 ng/ml phorbol 12-myristate 13-acetate (PMA, Sigma, USA) for 48 h to develop the morphology of differentiated macrophages. Then, medium was removed and replaced with fresh one. Macrophages were infected with 20 μl of AAV-DJ-hsa_circ_0004104 and AAV-DJ control (Jisai, China) for 48 h according to the manufacturer's protocol, respectively. mRNA expression profiling was performed with Agilent Human mRNA Microarray V6 (8*60 K, Design ID: 072363) by OE biotech Co., Ltd. (Shanghai, China) according to the manufacturer's procedures.

2.6. Enzyme-linked immunosorbent assay (ELISA)

Concentrations of MMP-8 and ApoA I in culture supernatants was measured with *in vitro* SimpleStep ELISA® (Enzyme-Linked Immunosorbent Assay) kit (ab219050, ab189576, Abcam, Cambridge, UK) according to manufacturer's instructions. Concentrations were calculated according to their corresponding standard curves.

2.7. Western blot analysis

Total protein was extracted using Cell lysis buffer (Beyotime, Nanjing, China). An equal amount of protein (10 mg) was loaded into 10% SDS polyacrylamide gel and electroblotted to NC membranes. The blots were blocked with 5% non-fat dry milk in TBS-T, and then incubated with anti-IDO1 antibody (ab211017), anti-CD40 antibody (ab224639), and anti- GAPDH antibody (ab181602) (Abcam, Cambridge, UK) at 4 °C overnight, respectively, followed by incubation with horseradish peroxidase-conjugated secondary antibody for 1 h at room temperature. Bands were revealed using a chemiluminescence kit (Thermo Scientific Pierce, Waltham, USA) and band density was quantified using Quantity One software (Bio-Rad Laboratories, CA, USA).

2.8. Statistical analysis

Categorical data are presented with count and percentile. Continuous variables are described as mean ± standard deviation. Student *t*-test was used to compare the demographic, clinical pathological characteristics and circRNAs expression levels between CAD patients and controls. Chi-squares were used to analyze the categorical data between two groups. Univariable and multivariable logistic regression analyses were conducted to evaluate whether circRNAs are independent factors for CAD. Spearman's correlation analysis was performed to investigate cardiac risk factors, conventional CAD markers, and cardiac function parameters related to circRNAs. The area under the receiver–operator characteristic (ROC) curve (AUC) was used to evaluate the diagnostic value of circRNAs for CAD. All analyses were carried out by R software (version 3.2.4; http://www.r-project.org). The significant level was set at 0.05 and two-tailed p values < 0.05 were considered statistically significant.

3. Results

3.1. Transcriptome-wide overview of aberrantly expressed circRNAs in CAD patients

A total of 170,340 circRNA targets were detected by microarray probes in peripheral blood mononuclear cells (PBMCs) in CAD patients (n = 24) and healthy controls (n = 7). Clinical and pathologic characteristics of samples undergoing circRNA expression profiling are presented in Supplementary Table 2. Hierarchical Clustering was performed to group circRNAs (Fig. 1A) and displayed the levels of circRNAs in CAD patients and healthy controls according to their expression levels among the samples, and the results indicated that circRNA expression profiles in CAD patients were distinctly different from those in healthy controls. The scatter plot visualizes fold changes (FC) of circRNA expression and identifies the differentially expressed circRNAs between CAD patients and healthy controls (Fig. 1B). The volcano plot shows the statistical significance of differentially expressed circRNAs (Fig. 1C) between CAD patients and healthy controls and identifies 795 circRNAs whose levels changed substantially (FC > 1.5), including 624 upregulated and 171 downregulated circRNAs, with statistical significance ($p < 0.05$). In the hierarchical clustering, scatter plot and volcano plot, red or green, represented upregulated or downregulated genes, respectively.

3.2. GO enrichment and KEGG pathway analysis

In order to assess potential regulation mechanisms of circRNAs in parental gene transcription, we conducted GO enrichment analysis. The result shows that genes targeted by the differential circRNAs are involved in the innate immune response, cell adhesion and cell migration (Supplementary Fig. 1A). KEGG analysis demonstrates that several pathways, such as metabolic pathways, PI3K-Akt signaling pathway, were related to the differential circRNAs (Supplementary Fig. 1A). In addition, we also conducted the network of related parental gene transcription with pathways. The results presented in Supplementary Fig. 1C reveal that PI3K-Akt was the most relevant process related to differential circRNAs.

3.3. Validation of differentially expressed circRNAs

To evaluate applicable biomarkers for CAD, we screened specific circRNA markers with high efficiency and the ability to identify CAD according to the expression levels. After using six different classifiers combining survival forest algorithms, we constructed a four-circRNA (hsa_circ_0001879, hsa_circ_0004104, hsa_circ_004432, hsa_circ_007142) signature. The diagnostic value of the four-circRNA signature in CAD is presented in Supplementary Table 3, indicating that the four-circRNA signature is capable of identifying CAD with 100% accuracy according to the expression levels in microarray stage.

To further assess the diagnostic value of circRNAs, we validated the expression levels of the four circRNAs by qRT-PCR in a large population (412 CAD patients and 290 controls). Clinical and pathologic characteristics of the validation sample are presented in Supplementary Table 2. The expression levels of circRNAs in PBMCs of CAD patients and controls are listed in Table 1. Hsa_circ_0001879 and hsa_circ_0004104 showed significant higher expression levels in CAD patients than controls ($p < 0.001$, Fig. 2A and B). However, there was no significant difference in hsa_circ_004432 or hsa_circ_007142 expression levels between the two groups ($p > 0.05$, Fig. 2C and D). Hsa_circ_0001879, located at chr9:107521543-107535189, was derived from Intron 4 of *NIPSNAP3A* gene, and hsa_circ_0004104, located at chr5:151043647-151049345, was derived from Exon 4–7 of *SPARC* gene. We focused on evaluating the diagnostic value of hsa_circ_0001879 and hsa_circ_0004104 as potential CAD biomarkers in further statistical analysis.

3.4. Correlation of hsa_circ_0001879 and hsa_circ_0004104 expression levels with clinical characteristics

To further investigate the potential value of hsa_circ_0001879 and hsa_circ_0004104 as CAD biomarkers, we conducted Spearman's rank correlation analysis to test whether hsa_circ_0001879 and hsa_circ_0004104 expression levels were correlated with cardiac risk factors, conventional CAD biomarkers. The results summarized in Table 2 showed that hsa_circ_0001879 expression level correlated with body mass index (BMI), SBP, DBP and Gensini score in CAD patients ($p < 0.05$), while the expression level of hsa_circ_0004104 correlated with HDL-C in CAD patients ($p < 0.05$). These results indicated that hsa_circ_0001879 and hsa_circ_0004104 might be involved in the pathogenesis of CAD.

3.5. Identification of hsa_circ_0001879 and hsa_circ_0004104 as independent predictors of CAD

Univariate and multivariate logistic regression was conducted to identify whether hsa_circ_0001879 and hsa_circ_0004104 could be predictors of CAD occurrence. As showed in Table 3, with a unit increase of hsa_circ_0001879 level, the odds ratio (OR) for CAD occurrence was 1.576 (95% CI: 1.289–1.926; $p < 0.001$) after adjusting for age, BMI, hypertension status, smoking, drinking, TC, LDL, fasting blood glucose and SBP. In addition, the adjusted OR was 2.527 (95% CI: 1.677–3.809; $p < 0.001$) with a unit increase of hsa_circ_0004104. The results imply that hsa_circ_0001879 and hsa_circ_0004104 might increase the risk of CAD.

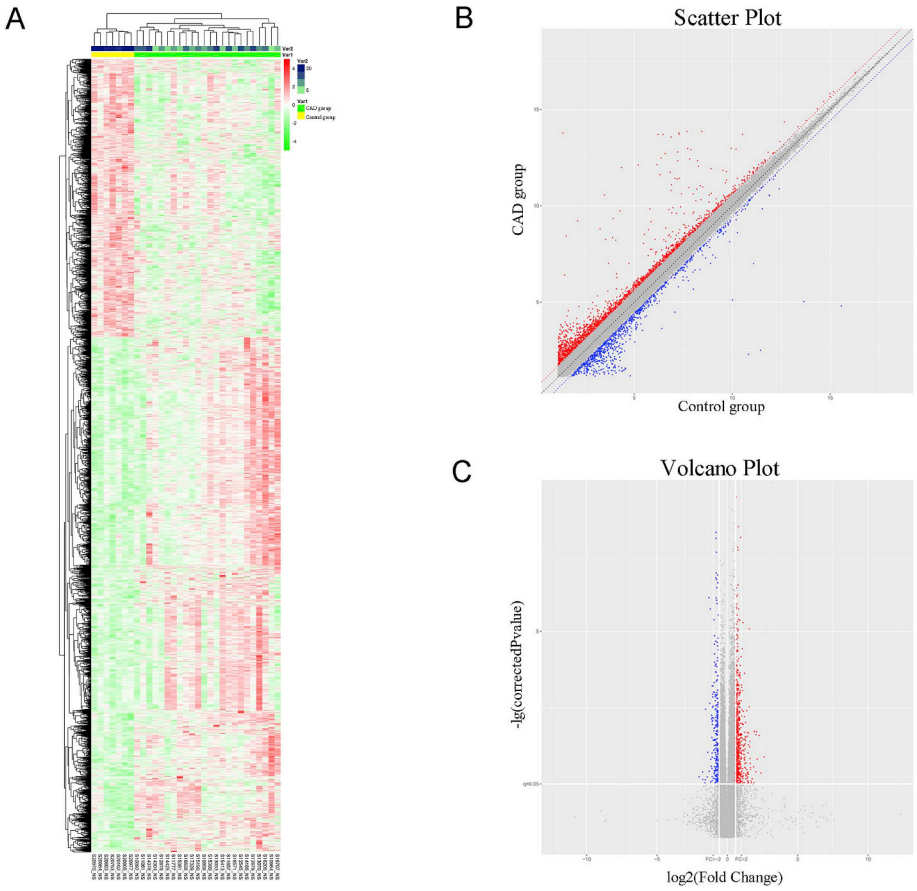

Fig. 1. Differentially expressed circular RNAs (circRNAs) between CAD patients and healthy controls.
(A) Heat map analysis of circRNA microarray profile in CAD patients (n = 24) and controls (n = 7). The expression of circRNAs is hierarchically clustered on the y-axis; CAD patients and controls are hierarchically clustered on the x-axis. Expression values are presented in red and green to indicate upregulation and downregulation, respectively. g134 indicates CAD patients and g2 controls. (B) Scatter plot. X-axis: controls (normalized), Y-axis: CAD patients (normalized). The red and blue lines represent fold change. The circRNAs above the red line and below the blue line indicate more than 2.0- fold change in circRNAs between CAD patients and controls. (C) Volcano plot. X-axis: log2 (fold change); Y-axis: log10 (*p*-value). The vertical white lines indicate 2.0 folds up and down, and the horizontal white line represents a *p*-value of 0.05. The red points indicate circRNAs 1.5 fold upregulated significantly and the blue points represent circRNAs 1.5 fold downregulated with statistical significance. (For interpretation of the references to color in this figure legend, the reader is referred to the Web version of this article.)

Table 1
The expression levels of circRNAs in validation population.

circRNAs	CAD group (n = 412)	Control group (n = 290)	Fold change	*p*
hsa_circ_0001879	1.63 ± 1.51	0.98 ± 1.25	1.66	< 0.001
hsa_circ_0004104	1.34 ± 1.03	0.74 ± 0.66	1.81	< 0.001
hsa_circ_004432	1.19 ± 0.92	1.12 ± 0.88	1.06	0.529
hsa_circ_007142	1.30 ± 0.94	1.11 ± 0.82	1.17	0.052

Data is expressed as mean ± standard deviation.

3.6. Evaluation of hsa_circ_0001879 and hsa_circ_0004104 as potential biomarkers for CAD

ROC analysis was performed to explore the diagnostic value of hsa_circ_0001879 and hsa_circ_0004104 in CAD patients and controls. The results in Fig. 3A and B showed that the AUC of hsa_circ_0001879 was 0.703 (95% CI: 0.656–0.750; $p < 0.001$), the sensitivity and specificity were 0.831 and 0.543, respectively. The AUC of hsa_circ_0004104 was 0.700 (95% CI: 0.646–0.755; $p < 0.001$), the sensitivity and specificity were 0.707 and 0.614, respectively. In addition, we conducted ROC analysis for the combination of the two circRNAs to test the diagnostic value of this combination for CAD. As Fig. 3C shows, the AUC was slightly higher (AUC: 0.742, 95% CI: 0.688–0.797; $p < 0.001$) when compared to each circRNA alone, while the sensitivity and specificity were 0.769 and 0.620, respectively. Furthermore, Fig. 3D shows that after introducing the risk factors and conventional marker for CAD (smoking, TC and serum creatinine), the AUC increased to 0.832 (95% CI: 0.788–0.876; $p < 0.001$), the sensitivity was 0.668 and the specificity was 0.890. The results showed that hsa_circ_0001879 and hsa_circ_0004104 could both serve as a potential biomarker for CAD. The combination of hsa_circ_0001879 and hsa_circ_0004104 did not have higher diagnostic value. However, the combination of the two circRNAs with CAD risk factors and conventional marker increased the value for CAD identification.

3.7. Influence of hsa_circ_0004104 overexpression in THP-1-derived macrophages

Gain-of-function approach was used to determine the influence of hsa_circ_0004104 overexpression on gene expression alterations of THP-1-derived macrophages. The expression of recombined plasmid K4ssAAV.CMV.GFP.WPRE-hsa_circ_0004104 in 293 T cells was verified by qRT-PCR and Sanger sequencing, and the result showed that hsa_circ_0004104 gene was successfully overexpressed as circRNA, with sequence of back-splicing junction site identical to the sequence in circbase (Fig. 4A). Then, AAV-DJ-mediated delivery of hsa_circ_0004104 into THP-1-derived macrophages led to relative higher expression of hsa_circ_0004104 (Fig. 4B), and overexpression of hsa_circ_0004104 altered gene expression profile assessed by mRNA microarray. The volcano plot shows the statistical significance of differentially expressed mRNAs between the AAV-hsa_circ_0004104 group and AAV-DJ group (Fig. 4C), and IPA indicated that among the top 10 function categories, differentially expressed mRNAs were involved in atherosclerosis signaling pathway, and inflammation related pathways, such as leukocyte extravasation signaling pathway (Fig. 4D). We selected differentially expressed mRNAs involved in these significant pathways or based on literature on cardiovascular disease. qRT-PCR confirmed that transcripts for proatherosclerotic genes, such as IDO1, MMP-8, CD40, were significantly up-regulated in the AAV-hsa_circ_0004104 group, and transcripts for antiatherosclerotic genes, such as ApoA I, RNASE1, were significantly down-regulated in the AAV-hsa_circ_0004104 group (Fig. 4E).

Corresponding to mRNA levels, IDO1 protein and CD40 protein

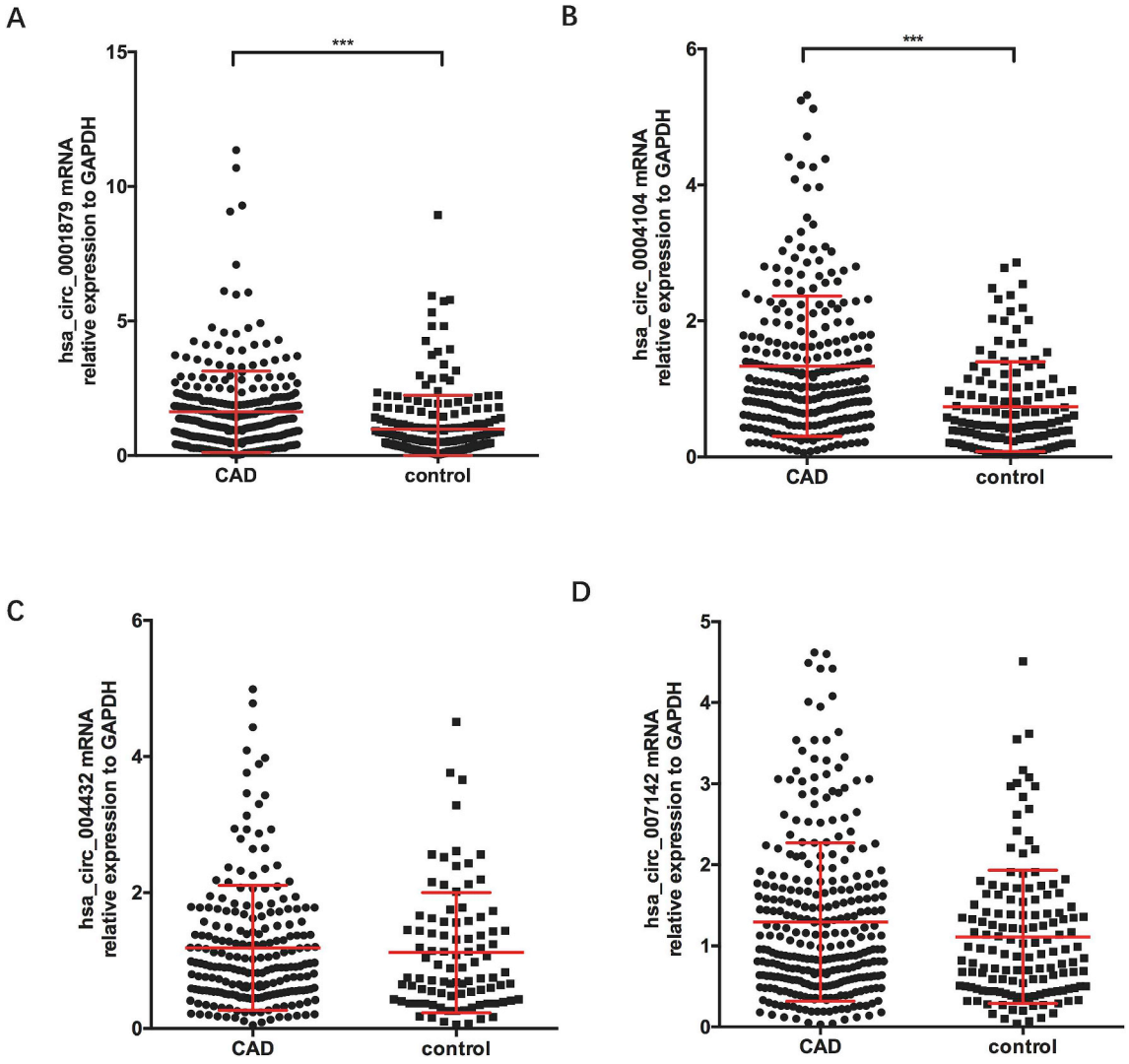

Fig. 2. qRT-PCR analysis of expression of 4 circRNAs in a large sample of CAD patients (n = 412) and healthy controls (n = 290).
(A) hsa_circ_0001879. (B) hsa_circ_0004104. (C) hsa_circ_004432. (D) hsa_circ_0007142. ***$p < 0.001$ *vs.* control group (two-tailed *t*-test).

Table 2
Correlation between baseline characteristic and circRNAs level in CAD patients.

Parameters	hsa_circ_0001879		hsa_circ_0004104	
	Coefficient	*p*	Coefficient	*p*
Age (years)	0.015	0.784	−0.018	0.777
BMI (kg/m^2)	0.115	0.045*	−0.006	0.922
SBP (mmHg)	0.135	0.017*	0.009	0.888
DBP (mmHg)	0.167	0.003*	−0.035	0.577
Hypertension	0.026	0.649	0.011	0.854
Smoking	0.068	0.227	−0.010	0.869
Drinking	−0.084	0.139	−0.037	0.551
TC (mg/dL)	−0.023	0.686	−0.040	0.518
TG (mg/dL)	0.068	0.233	−0.126	0.151
HDL-C (mg/dL)	−0.088	0.121	−0.147	0.018*
LDL-C (mg/dL)	−0.027	0.629	−0.042	0.500
Fasting blood glucose (mg/dL)	−0.088	0.122	−0.107	0.083
Serum creatinine (μmol/L)	0.003	0.955	−0.052	0.398
CKMB (ng/mL)	−0.040	0.480	−0.099	0.109
Gensini score	0.134	0.027*	−0.055	0.400

*$p < 0.05$.
BMI: body mass index; SBP: systolic blood pressure; DBP: diastolic blood pressure; TC: total cholesterol; TG: triacylglycerol; HDL-C: high-density lipoprotein cholesterol; LDL-C: low-density lipoprotein cholesterol; CKMB: creatine kinase-myocardial band.

were drastically up-regulated in the AAV-hsa_circ_0004104 group (Fig. 5A and B), MMP-8 protein levels in culture supernatants of the AAV-hsa_circ_0004104 group detected using ELISA was significantly increased, compared with the control group (Fig. 5C), and ApoA I protein levels in culture supernatants of the AAV-hsa_circ_0004104 group was significantly decreased, compared with that of the control group (Fig. 5D). The results confirmed a role for the overexpression of hsa_circ_0004104 in positively regulating proatherosclerotic genes expression and negatively regulating antiatherosclerotic genes expression in THP-1-derived macrophages, indicating a potential proatherosclerotic effect of the upregulation of hsa_circ_0004104 in the pathogenesis of atherosclerosis.

4. Discussion

In the present study, we first profiled circRNAs expression in the peripheral blood of CAD patients and controls. By means of computational analysis, we selected four candidate circRNAs to explore their diagnostic value as CAD biomarkers in large cohorts. Hsa_circ_0001879 and hsa_circ_0004104 were validated to be significantly upregulated in CAD patients. The AUC of hsa_circ_0001879 and hsa_circ_0004104 were 0.703 and 0.700, respectively. Moreover, the Spearman's correlation test demonstrated that hsa_circ_0001879 significantly correlated with

Table 3
Univariate and multivariate logistic regression analysis to identify circRNAs as independent predictors of CAD.

Variable	hsa_circ_0001879				hsa_circ_0004104			
	OR	95% CI		*p*	OR	95% CI		*p*
		lower	upper			lower	upper	
Univariate analysis	1.555	1.298	1.862	< 0.001	2.553	1.826	3.571	< 0.001
Multivariate logistic regression model 1	1.536	1.281	1.843	< 0.001	2.684	1.881	3.831	< 0.001
Multivariate logistic regression model 2	1.490	1.240	1.790	< 0.001	2.610	1.829	3.726	< 0.001
Multivariate logistic regression model 3	1.507	1.242	1.829	< 0.001	2.401	1.605	3.592	< 0.001
Multivariate logistic regression model 4	1.576	1.289	1.926	< 0.001	2.527	1.677	3.809	< 0.001

Model1 included age, BMI.
Model2 included age, BMI, smoking, drinking.
Model3 included age, BMI, hypertension, smoking, drinking, TC, LDL.
Model4 included age, BMI, hypertension, smoking, drinking, TC, LDL, fasting blood glucose, SBP.
OR: odds ratio; CI: confidence interval.

blood pressure and hsa_circ_0004104 negatively correlated with HDL-C, implying that hsa_circ_0001879 and hsa_circ_0004104 might be deeply involved in the pathologies of CAD. Our data show hsa_circ_0001879 and hsa_circ_0004104 could be used as novel circRNA biomarker for diagnosing CAD.

CAD is a multifactorial disease with high morbidity and mortality, causing a huge burden on social economies. The identification of early biomarkers for CAD should be part of risk prediction. CircRNAs may be generated from exonic or intronic sequences that are abundant in body fluids [14]. CircRNA is more stable than linear RNA because of the circular structure and resistance to RNA exonuclease, which makes it a better biomarker in human diseases. There is growing evidence of circRNA biomarkers in various cancers [11,13,15,16]. Up to now, only hsa_circ_0124644 and hsa-circ-11783-2 were reported to be used as potential diagnostic biomarkers for CAD [17,18], and circRNA MICRA improved risk classification after myocardial infarction, supporting the added value of this novel biomarker in future prognostication strategies [19], indicating that circRNAs have the potential to improve the

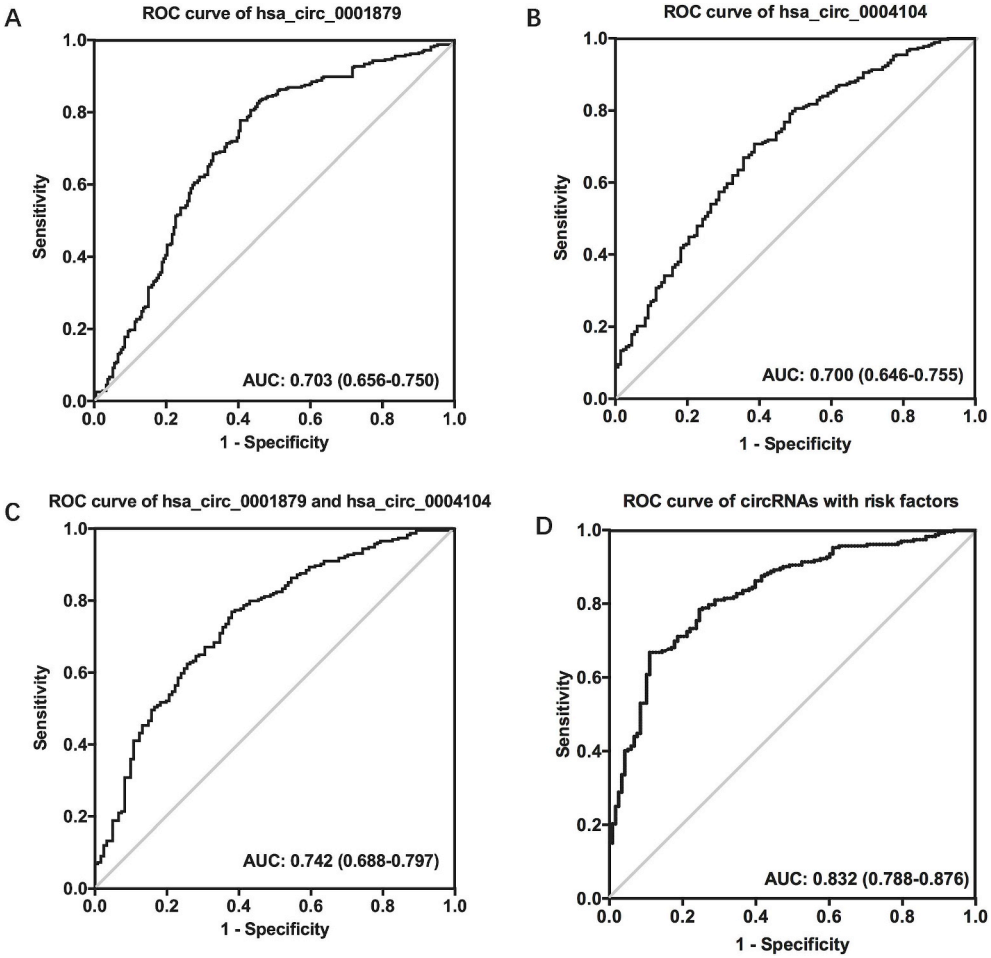

Fig. 3. ROC curve analysis of circRNAs for discrimination of CAD patients (n = 412) from healthy controls (n = 290).
(A) ROC of hsa_circ_0001879. (B) ROC of hsa_circ_0004104. (C) ROC of hsa_circ_0001879 with hsa_circ_0004104. (D) ROC of hsa_circ_0001879 and hsa_circ_0004104 combining CAD risk factors.

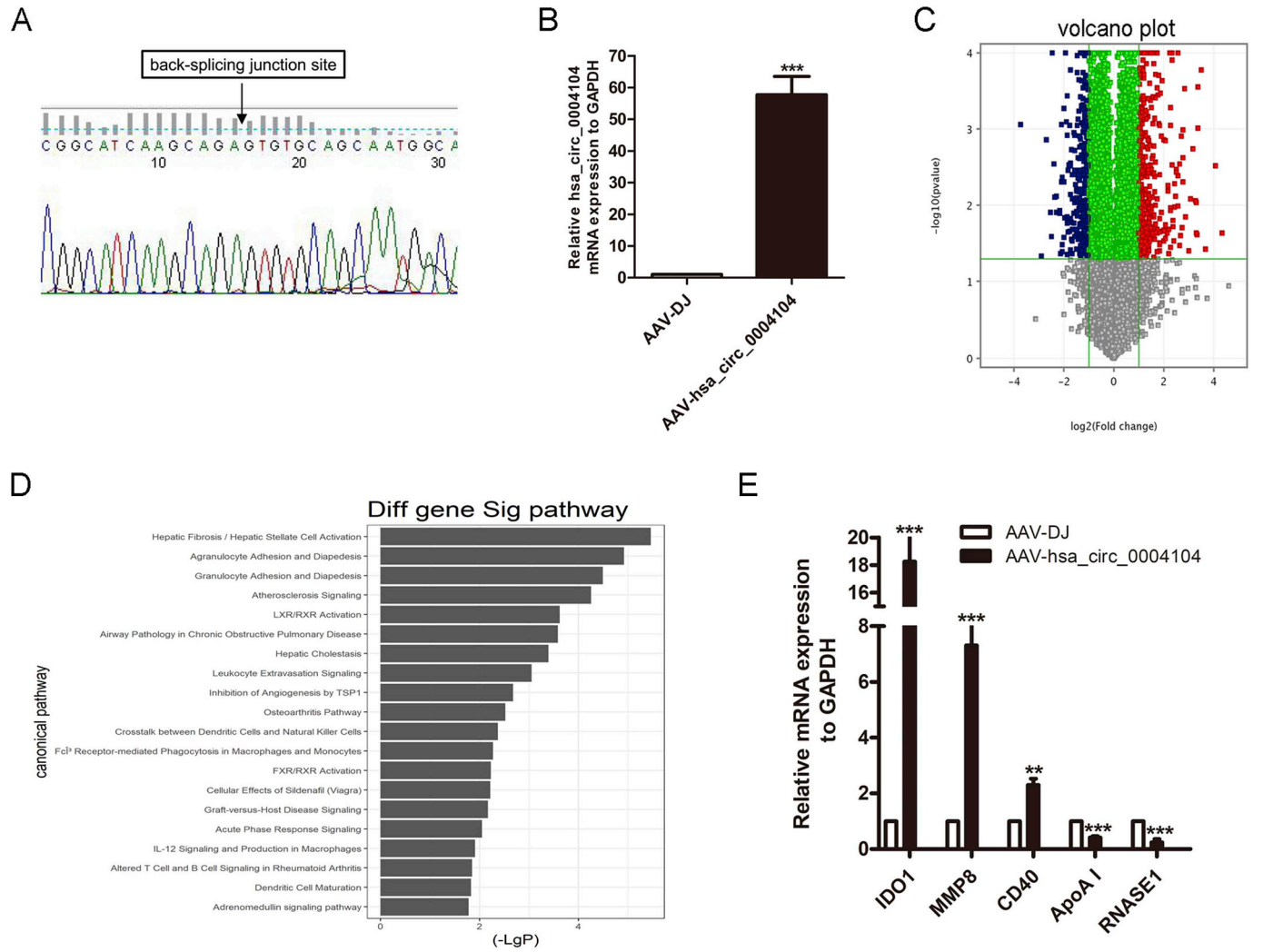

Fig. 4. Influence of hsa_circ_0004104 overexpression in THP-1-derived macrophages.
(A) The verification of sequence in the back-splicing junction site of hsa_circ_0004104 by qRT-PCR and Sanger sequencing. (B) qRT-PCR analysis of overexpression efficiency of AAV-DJ-hsa_circ_0004104 after infection for 48 h in THP-1-derived macrophages. (C) Volcano plot of differentially expressed mRNAs between the AAV-DJ -hsa_circ_0001879 group and AAV-DJ-GFP group assessed by mRNA microarray. (D) Top 10 canonical pathways of differentially expressed mRNAs. (E) qRT-PCR validation of differentially expressed mRNAs involved in these significant pathways or based on literature about cardiovascular disease. Data are presented as represent mean ± standard error. $^{**}p < 0.01$ and $^{***}p < 0.001$ *vs.* the control group. Each experiment was performed three times.

diagnosis and prognosis of CAD. However, the expression profile, biological functions and diagnostic value of circRNAs in CAD remain to be extensively investigated. We performed GO analysis to investigate the enriched GO of differentially expressed circRNAs. The results showed that differentially expressed circRNAs were involved in innate immune response, cell adhesion and cell migration. Mounting evidence showed that innate immune response was involved in the pathogenesis of CAD [20–22]. CAD risk factors triggered activation of circulating innate immune cells, and promoted leukocyte adhesion and migration to vascular endothelium, and phenotype transformation of smooth muscle cells from contractile to synthetic phenotype, both playing essential roles in the onset of atherosclerosis [23,24]. KEGG pathway analysis revealed that differentially expressed circRNAs were involved in metabolic pathways and PI3K-Akt signaling pathway. Previous studies showed that glucose metabolic pathway perturbation was the downstream mediator for cardiovascular diseases onset [25]. PI3K/Akt signaling pathway could be involved in metabolic regulation, activation of hypertrophy and survival pathways and its activation could be interconnected to activation of Ca^{2+} signaling, which is crucial for cells of the cardiovascular system by balancing contractility [26]. Furthermore, we combined the parental gene transcription with related pathways, indicating a similar result that PI3K/Akt signaling pathway was the most relevant process.

In addition, current complementary methods of diagnosing CAD include routine electrocardiogram (ECG), Holter monitoring, treadmill exercise test (TET), and coronary computed tomography angiography (CTA). The sensitivities of these methods have been shown to be 0.29 [27], 0.65 [28], 0.79 [29] and 0.92 [30], respectively. The specificities are 0.67 [27], 0.90 [28], 0.80 [29] and 0.75 [30], respectively. In our study, the sensitivity and specificity of hsa_circ_0001879 were 0.83 and 0.54, respectively. The sensitivity and specificity of hsa_circ_0004104 were 0.71 and 0.61, respectively. The diagnostic value of hsa_circ_0001879 and hsa_circ_0004104 was greater than that of routine ECG, and approximately equal to that of Holter monitoring, TET and CTA. When combined with CAD risk factors and conventional markers, the diagnostic value of hsa_circ_0001879 and hsa_circ_0004104 was even higher. Considering the cost and convenience of diagnostic methods, hsa_circ_0001879 and hsa_circ_0004104 might ameliorate the diagnosis of CAD.

The linear length of hsa_circ_0001879 exceeds 10 thousand bps, so it is not feasible to overexpress hsa_circ_0001879 in cells. Then we explored the functional significance of hsa_circ_0004104 in THP-1-

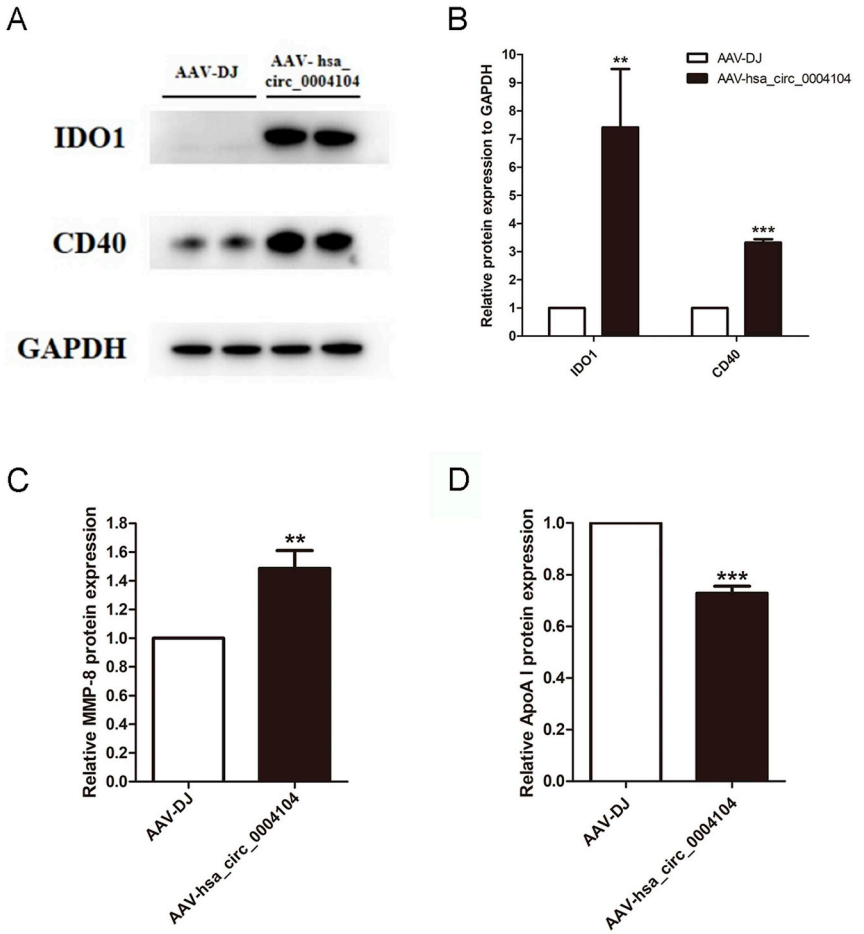

Fig. 5. The effect of hsa_circ_0004104 overexpression on protein expression of *IDO1*, *MMP8, CD40* and *ApoA I* genes in THP-1-derived macrophages.
(A and B) IDO1 and CD40 proteins in the AAV-hsa_circ_0004104 and AAV-DJ groups were detected by Western blot and normalized to GAPDH level; (C) MMP-8 protein level in culture supernatants in the AAV-hsa_circ_0004104 and AAV-DJ groups was detected by ELISA; (D) ApoA I protein level in culture supernatants in the AAV-hsa_circ_0004104 and AAV-DJ groups was detected by ELISA. Data are presented as mean ± standard error. $^{**}p < 0.01$ and $^{***}p < 0.001$ *vs.* the control group. Each experiment was performed three times.

derived macrophages using a gain-of-function approach. We successfully overexpressed hsa_circ_0004104 in THP-1-derived macrophages through the AAV-DJ system, and determined gene expression pattern altered by the overexpression of hsa_circ_0004104 using mRNA microarray, qRT-PCR validation and Western blot or ELISA. Among the dysregulated genes, indoleamine 2,3-dioxygenase 1 (IDO1) is a rate-limiting enzyme that catalyzes the degradation of tryptophan along the kynurenine pathway, and the absence of Ido1 protects against atherosclerosis through increase of IL-10 [31]. MMP8, one member of the family of zinc-dependent proteases, belonging to the metzincin superfamily [32], is involved in atherosclerosis pathogenesis and progression, atherosclerotic plaque destabilization, neointima formation following vascular injury, and abdominal aortic aneurysm development and expansion [33–35]. Soluble CD40 ligand promotes macrophage foam cell formation in the etiology of atherosclerosis [36], and targeting CD40-induced TRAF6 signaling in macrophages reduces atherosclerosis [37]. Apolipoprotein AI (ApoA I) is the major protein component of HDL, and transgenic mice with high plasma ApoA I and HDL levels are significantly protected from the development of fatty streak lesions [38]. Recombinant ApoA I Milano/phospholipid complex (ETC-216), administered intravenously for 5 doses at weekly intervals, produces significant regression of coronary atherosclerosis [39]. Upregulation of ApoA I expression contributes to the reduction of atherosclerosis by KLF14 activated by perhexiline [40]. Extracellular RNA (eRNA) is involved in high-fat diet-induced atherosclerosis and neointima formation after injury in atherosclerosis-prone mice, while RNASE1 could function as natural antagonists of eRNA [41]. Treatment with RNase1 not only diminished the increased plasma level of eRNA evidenced after injury, but also reduced neointima formation in comparison with vehicle-treated $ApoE^{-/-}$ controls and was associated with a significant decrease in plaque macrophage content in a model of accelerated atherosclerosis after arterial injury in $ApoE^{-/-}$ mice [42]. Therefore, upregulation of atherosclerosis-susceptible genes, such as *IDO1, MMP8, CD40*, and downregulation of anti-atherosclerosis genes, such as *ApoA I, RNASE1*, by overexpression of hsa_circ_0004104 in THP-1-derived macrophages indicates that the upregulation of hsa_circ_0004104 in CAD patients might contribute to the pathogenesis of atherosclerosis and CAD.

It should be noted that there are some limitations in our study. For their utility as biomarkers for diagnosing CAD, hsa_circ_0001879 and hsa_circ_0004104 should be further validated across different clinical settings. Due to the lack of follow-up information for CAD patients, prognostic values of these two circRNA biomarkers in major cardiovascular events (MACE) should be evaluated in subsequent studies. Compared with RNA-seq, circRNA microarray does not allow for *de novo* circRNAs identification for the principle of designing probes based on sequences of existing circRNAs.

In summary, this study offered a transcriptome-wide overview of aberrantly expressed circRNAs in CAD patients and identified hsa_circ_0001879 and hsa_circ_0004104 as novel circRNA biomarkers to diagnose CAD. Finally, we discerned the function of hsa_circ_0004104 in THP-1-derived macrophages. In future studies, we will focus on the roles and underlying mechanisms of hsa_circ_0004104 in the pathogenesis of atherosclerosis and CAD.

Conflicts of interest

The authors declared they do not have anything to disclose regarding conflict of interest with respect to this manuscript.

Financial support

This work was supported by CAMS Innovation Fund for Medical Sciences(CIFMS)(No.2016-I2M-1-009 to LYW; 2017-I2M-1-004 to DFG; 2016-I2M-1-011 to XFL; 2016-I2M-2-001 to SFC; 2016-I2M-3-018 to JCC), Grants from National Natural Science Foundation of China (No.91439202 to DFG), the Opening Foundation of State Key Laboratory of Cardiovascular Disease (2016kf-06 to LYW), and the High-Tech Research and Development Program of China (863 Plan; 2012AA02A516 to DFG) from the Ministry of Science and Technology of China.

Author contributions

Laiyuan Wang, Tianyu Zou and Chong Shen analyzed the data and wrote this manuscript. Yanyu Wang, Huijuan Zhu and Xiaomei Lu performed the experiment of circRNA expression levels. Lin Li, Bin Yang, Jichun Chen, Shufeng Chen and Xiangfeng Lu monitored the quality of experiments and checked the programs of statistical analysis. Laiyuan Wang and Dongfeng Gu conceived and designed the study, and supervised all the sample selection, data analysis and interpretation. All authors read and approved the final manuscript.

Acknowledgements

We sincerely thank all patients and healthy volunteers who participated in this study.

Appendix A. Supplementary data

Supplementary data to this article can be found online at https://doi.org/10.1016/j.atherosclerosis.2019.05.006.

References

[1] S. Negi, A. Anand, Atherosclerotic coronary heart disease-epidemiology, classification and management, Cardiovasc. Haematol. Disord. - Drug Targets 10 (2010) 257–261.
[2] S.W. Waldo, E.A. Secemsky, C. O'Brien, et al., Surgical ineligibility and mortality among patients with unprotected left main or multivessel coronary artery disease undergoing percutaneous coronary intervention, Circulation 130 (2014) 2295–2301.
[3] Z. Li, C. Huang, C. Bao, et al., Exon-intron circular RNAs regulate transcription in the nucleus, Nat. Struct. Mol. Biol. 22 (2015) 256–264.
[4] W.R. Jeck, J.A. Sorrentino, K. Wang, et al., Circular RNAs are abundant, conserved, and associated with ALU repeats, RNA (N. Y.) 19 (2013) 141–157.
[5] S. Memczak, M. Jens, A. Elefsinioti, et al., Circular RNAs are a large class of animal RNAs with regulatory potency, Nature 495 (2013) 333–338.
[6] T.B. Hansen, T.I. Jensen, B.H. Clausen, et al., Natural RNA circles function as efficient microRNA sponges, Nature 495 (2013) 384–388.
[7] H.H. Geng, R. Li, Y.M. Su, et al., The circular RNA Cdr1as promotes myocardial infarction by mediating the regulation of miR-7a on its target genes expression, PLoS One 11 (2016) e0151753.
[8] K. Wang, B. Long, F. Liu, et al., A circular RNA protects the heart from pathological hypertrophy and heart failure by targeting miR-223, Eur. Heart J. 37 (2016) 2602–2611.
[9] H. Xie, X. Ren, S. Xin, et al., Emerging roles of circRNA_001569 targeting miR-145 in the proliferation and invasion of colorectal cancer, Oncotarget 7 (2016) 26680–26691.
[10] M. Qin, G. Liu, X. Huo, et al., Hsa_circ_0001649: a circular RNA and potential novel biomarker for hepatocellular carcinoma, Cancer Biomark. : section A of Disease markers 16 (2016) 161–169.
[11] P. Li, S. Chen, H. Chen, et al., Using circular RNA as a novel type of biomarker in the screening of gastric cancer, Clinica chimica acta, Int. J. Clin. Chem. 444 (2015) 132–136.
[12] M. Huang, Z. Zhong, M. Lv, et al., Comprehensive Analysis of Differentially Expressed Profiles of lncRNAs and circRNAs with Associated Co-expression and ceRNA Networks in Bladder Carcinoma, Oncotarget, 2016.
[13] X. Shang, G. Li, H. Liu, et al., Comprehensive circular RNA profiling reveals that hsa_circ_0005075, a new circular RNA biomarker, is involved in hepatocellular crcinoma development, Medicine 95 (2016) e3811.
[14] X. Fan, X. Weng, Y. Zhao, et al., Circular RNAs in cardiovascular disease: an overview, BioMed Res. Int. 2017 (2017) 5135781.
[15] X. Jin, C.Y. Feng, Z. Xiang, et al., CircRNA expression pattern and circRNA-miRNA-mRNA network in the pathogenesis of nonalcoholic steatohepatitis, Oncotarget 7 (2016) 66455–66467.
[16] L. Lu, J. Sun, P. Shi, et al., Identification of Circular RNAs as a Promising New Class of Diagnostic Biomarkers for Human Breast Cancer, Oncotarget, 2017.
[17] Z. Zhao, X. Li, C. Gao, et al., Peripheral blood circular RNA hsa_circ_0124644 can be used as a diagnostic biomarker of coronary artery disease, Sci. Rep. 7 (2017) 39918.
[18] X. Li, Z. Zhao, D. Jian, et al., Hsa-circRNA11783-2 in peripheral blood is correlated with coronary artery disease and type 2 diabetes mellitus, Diabetes Vasc. Dis. Res. 14 (2017) 510–515.
[19] P.M. Ridker, T.F. Luscher, Anti-inflammatory therapies for cardiovascular disease, Eur. Heart J. 35 (2014) 1782–1791.
[20] R.M. Hoogeveen, M. Nahrendorf, N.P. Riksen, et al., Monocyte and haematopoietic progenitor reprogramming as common mechanism underlying chronic inflammatory and cardiovascular diseases, Eur. Heart J. 39 (38) (2018) 3521–3527.
[21] I. Tabas, A.H. Lichtman, Monocyte-Macrophages and T Cells in atherosclerosis, Immunity 47 (2017) 621–634.
[22] V.R. Taqueti, M.F. Di Carli, M. Jerosch-Herold, et al., Increased microvascularization and vessel permeability associate with active inflammation in human atheromata, Circulation. Cardiovascular imaging 7 (2014) 920–929.
[23] S.S. Rho, K. Ando, S. Fukuhara, Dynamic regulation of vascular permeability by vascular endothelial cadherin-mediated endothelial cell-cell junctions, J. Nippon Med. Sch. 84 (2017) 148–159 Nippon Ika Daigaku zasshi.
[24] M.R. Bennett, S. Sinha, G.K. Owens, Vascular smooth muscle cells in atheJ. Nippon Med. Sch.rosclerosis, Circ. Res. 118 (2016) 692–702.
[25] R.F. Mapanga, M.F. Essop, Damaging effects of hyperglycemia on cardiovascular function: spotlight on glucose metabolic pathways, Am. J. Physiol. Heart Circ. Physiol. 310 (2016) H153–H173.
[26] A. Ghigo, M. Laffargue, M. Li, et al., PI3K and calcium signaling in cardiovascular disease, Circ. Res. 121 (2017) 282–292.
[27] B. Ghadrdoost, M. Haghjoo, A. Firouzi, Accuracy of cardiogoniometry compared with electrocardiography in the diagnosis of coronary artery disease, Res. Cardiovasc. Med. 4 (2015) e25547.
[28] Y. Jiang, J.P. Tian, H. Wang, et al., Diagnostic value of combined parameters derived from ambulatory electrocardiography for detecting coronary artery disease in non-active chest pain patients, Pakistan J. Med. Sci. 30 (2014) 1331–1335.
[29] J.L. Sun, R. Han, J.H. Guo, et al., The diagnostic value of treadmill exercise test parameters for coronary artery disease, Cell Biochem. Biophys. 65 (2013) 69–76.
[30] A. Arbab-Zadeh, M.F. Di Carli, R. Cerci, et al., Accuracy of computed tomographic angiography and single-photon emission computed tomography-acquired myocardial perfusion imaging for the diagnosis of coronary artery disease, circulation, Cardiovasc. Imaging 8 (2015) e003533.
[31] S. Metghalchi, P. Ponnuswamy, T. Simon, et al., Indoleamine 2,3-dioxygenase fine-tunes immune homeostasis in atherosclerosis and colitis through Repression of interleukin-10 production, Cell Metabol. 22 (2015) 460–471.
[32] H. Nagase, R. Visse, G. Murphy, Structure and function of matrix metalloproteinases and TIMPs, Cardiovasc. Res. 69 (2006) 562–573.
[33] S. Ye, Putative targeting of matrix metalloproteinase-8 in atherosclerosis, Pharmacol. Therapeut. 147 (2015) 111–122.
[34] J. Lin, V. Kakkar, X. Lu, Impact of matrix metalloproteinases on atherosclerosis, Curr. Drug Targets 15 (2014) 442–453.
[35] S. Lenglet, F. Mach, F. Montecucco, Role of Matrix Metalloproteinase-8 in Atherosclerosis, Mediat. Inflamm. vol. 2013, (2013) 659282.
[36] M. Yuan, H. Fu, L. Ren, et al., Soluble CD40 ligand promotes macrophage foam cell formation in the etiology of atherosclerosis, Cardiology 131 (2015) 1–12.
[37] T.T.P. Seijkens, C.M. van Tiel, P.J.H. Kusters, et al., Targeting CD40-induced TRAF6 signaling in macrophages reduces atherosclerosis, J. Am. Coll. Cardiol. 71 (2018) 527–542.
[38] E.M. Rubin, R.M. Krauss, E.A. Spangler, et al., Inhibition of early atherogenesis in transgenic mice by human apolipoprotein AI, Nature 353 (1991) 265–267.
[39] S.E. Nissen, T. Tsunoda, E.M. Tuzcu, et al., Effect of recombinant ApoA-I Milano on coronary atherosclerosis in patients with acute coronary syndromes: a randomized controlled trial, Jama 290 (2003) 2292–2300.
[40] Y. Guo, Y. Fan, J. Zhang, et al., Perhexiline activates KLF14 and reduces atherosclerosis by modulating ApoA-I production, J. Clin. Investig. 125 (2015) 3819–3830.
[41] A. Zernecke, K.T. Preissner, Extracellular Ribonucleic acids (RNA) enter the stage in cardiovascular disease, Circ. Res. 118 (2016) 469–479.
[42] S. Simsekyilmaz, H.A. Cabrera-Fuentes, S. Meiler, et al., Role of extracellular RNA in atherosclerotic plaque formation in mice, Circulation 129 (2014) 598–606.